Poly(oxyalkylene)diamine-Functionalized Carbon Nanotube/Perfluorosulfonated Polymer Composites: Synthesis, Water State, and Conductivity

Wei-Fu Chen, Jing-Sin Wu, and Ping-Lin Kuo*

Department of Chemical Engineering, National Cheng Kung University, Tainan, Taiwan 70101

Received January 14, 2008. Revised Manuscript Received June 16, 2008

A new class of organic−inorganic composite membranes has been constructed, as proton exchange electrolytes, in which the structures of the composites have been designed at the molecular scale to possess fast proton conduction. Polysiloxane-functionalized multiwall carbon nanotubes (CNTs) were synthesized by covalently grafting hydrophilic layers composed of poly(oxyalkylene)diamines and tetraethyl orthosilicate-reinforced polysiloxane in a layer-by-layer manner onto the tube walls. The modified carbon nanotubes were blended with Nafion to form a proton-conducting membrane. Scanning electron microscopy images showed that the functionalized nanotubes had a better dispersion than the unfunctionalized nanotubes on the composite fracture surfaces. The incorporation of the inorganic polysiloxane layer onto the CNT sidewalls forms a resistance, which effectively prohibits electron conduction between the nanotubes. The incorporation of the amino-containing polymer onto the CNTs promotes Nafion coalescence on the CNTs through ionic interactions between amines and sulfonate groups, as evidenced by the shift of the $-SO_3^-$ symmetric stretching peak in the FTIR, the N 1s region in X-ray photoelectron spectroscopy, and the increase of the decomposition temperature of sulfonate groups in thermogravimetric analysis. This approach provides continuous paths suitable for fast proton conduction ($\sigma = 2.8 \times 10^{-2}$ S/cm at 30 °C) and also maintains the proton conduction at high temperatures ($\sigma = 6.3 \times 10^{-2}$ S/cm at 130 °C).

Introduction

Carbon nanotubes (CNTs) currently attract scientific and technological attention because of their exceptional properties and their consequent emerging applications in nanoelectronics and in the field of nanocomposites.[1−3] It is widely recognized that the fabrication of high-performance nanotube/polymer composites depends on the efficient load transfer from the host matrix to the tubes. The load transfer requires homogeneous dispersion of the filler and strong interfacial bonding between the two components.[4] To address these issues, several strategies for the synthesis of such composites have been developed. Currently, these strategies include physical mixing in solution,[5−7] in situ polymerization of monomers in the presence of nanotubes,[8] and the surfactant-assisted processing of composites.[9−13]

Perfluorosulfonate ionomers, such as Nafion, are being extensively studied for their potential applications in sensors and also as materials for polymer electrolyte membrane fuel cells (PEMFCs). Nafion is currently the best performing cation-exchange membrane because of its unique ion-exchange properties, chemical and mechanical stability, and high proton conductivity. However, further progress is still needed to enhance the membrane performance in terms of permselectivity, water management, and proton conduction at high temperatures. For these reasons, researchers have synthesized and studied modifications to Nafion membranes, by using inorganic fillers such as SiO_2,[14] nanoclay,[15] inorganic particles,[16] and a polymer hybrid.[17−19]

Recently, Nafion has been used for the successful dispersion of CNTs.[20,21] The components were mixed in solution, and the resulting blends, which were found to behave as potential actuators, have been widely used in the development and construction of sensors and electrodes. However, areas of application that seek to incorporate CNTs as polymer composite reinforcements, with a CNT content higher than

* To whom correspondence should be addressed. Phone: +886-6-275 7575-62658. Fax: +886-6-276 2331. E-mail: plkuo@mail.ncku.edu.tw.

(1) Andrews, R.; Jacques, D.; Qian, D.; Rantell, T. *Acc. Chem. Res.* **2002**, *35*, 1008.
(2) Sun, Y.-P.; Fu, K.; Lin, Y.; Huang, W. *Acc. Chem. Res.* **2002**, *35*, 1096.
(3) Ajayan, P. M. *Chem. Rev.* **1999**, *99*, 1787.
(4) Thess, A.; Lee, R.; Nikolaev, P.; Dai, H.; Petit, P.; Robert, J.; Xu, C.; Lee, Y. H.; Kim, S. G.; Rinzler, A. G.; Colbert, D. T.; Scuseria, G. E.; Tománek, D.; Fischer, J. E.; Smalley, R. E. *Science* **1996**, *273*, 483.
(5) Holzinger, M.; Vostrowsky, O.; Hirsh, A.; Hennrich, F.; Kappes, M.; Weiss, R.; Jellen, F. *Angew. Chem., Int. Ed.* **2001**, *40*, 4002.
(6) Riggs, J. E.; Guo, Z.; Carroll, D. L.; Sun, Y.-P. *J. Am. Chem. Soc.* **2000**, *122*, 5879.
(7) Zhu, J.; Yudasaka, M.; Zhang, M.; Kasuya, D.; Iijima, S. *Nano Lett.* **2003**, *3*, 1239.
(8) Tasis, D.; Tagmatarchis, N.; Bianco, A.; Prato, M. *Chem. Rev.* **2006**, *106*, 1105.
(9) Moore, V. C.; Strano, M. S.; Haroz, E. H.; Hauge, R. H.; Smalley, R. H. *Nano Lett.* **2003**, *3*, 1379.
(10) Matarredona, O.; Rhoads, H.; Li, Z.; Harwell, J. H.; Balzano, L.; Resasco, D. E. *J. Phys. Chem. B* **2003**, *107*, 13357.
(11) Yurekli, K.; Mitchell, C. A.; Krishnamoorti, R. *J. Am. Chem. Soc.* **2004**, *126*, 9902.
(12) Bachilo, S. M.; Strano, M. S.; Kittrell, C.; Hauge, R. H.; Smalley, R. E.; Weisman, R. B. *Science* **2002**, *298*, 2361.
(13) O'Connell, M. J.; Bachilo, S. M.; Huffman, C. B.; Moore, V. C.; Strano, M. S.; Haroz, E. H.; Rialon, K. L.; Boul, P. J.; Noon, W. H.; Kittrell, C.; Ma, J.; Hauge, R. H.; Weisman, R. B.; Smalley, R. E. *Science* **2002**, *297*, 593.

10.1021/cm8001354 CCC: $40.75
Published on Web 08/22/2008

5 wt %, have been beset by a number of critical problems.[22,23] Because of strong intrinsic van der Waals forces, CNTs tend to hold together as ropes and bundles, and as a consequence they have very low solubility in most solvents, leading to poor dispersion when mixed into the polymer matrix. Moreover, the atomically smooth surface of the nanotubes, and lack of interfacial bonding, limits load transfer from the polymer matrix to the nanotubes. Therefore, the ability to disperse high concentrations of the CNTs homogeneously inside the polymer matrix, as well as the ability to produce a strong interfacial interaction between the CNTs and the polymers, will be key issues that must be addressed to maximize the advantages of CNT reinforcement.

In this research, a new type of organic−inorganic nanocomposite was constructed as a proton exchange electrolyte for fuel cell applications, in which the structures of the composite have been designed at the molecular scale to possess fast proton conduction. We have synthesized polysiloxane-functionalized multiwall carbon nanotubes (CNTs) by covalently grafting a hydrophilic layer composed of poly(oxyalkylene)diamines (XTJ-511) and a tetraethyl orthosilicate (TEOS)-reinforced polysiloxane layer onto the tube walls. The modified carbon nanotubes were blended with Nafion to form a proton-conducting membrane. We postulated that the incorporation of an amino-containing polymer onto CNTs would help Nafion to coalesce strongly on the CNTs through electrostatic interactions between the amine and the sulfonate groups, thereby providing continuous paths suitable for fast proton conduction as shown in Scheme 1. In addition to acting as a robust scaffold, the polysiloxane's backbone also provides bonding sites for hydrogen bonding with water. The hydroxyl and amino functionalities and silica nodes allow the formation of a bound water layer that facilitates the hopping of protons as shown in Scheme 2. The CNT/Nafion nanocomposites were extensively characterized to understand how the layered structure of the composite membrane affects its hydrocharacteristics. The method described here is designed to reduce the short-range attraction between adjacent tubes, via the interactions of repulsive forces of similar strengths. Consequently, this treatment leads to modifications of the structural, electronic, and chemical properties of the tubes.

(14) Ladewig, B. P.; Knott, R. B.; Hill, A. J.; Riches, J. D.; White, J. W.; Martin, D. J.; Diniz da Costa, J. C.; Lu, G. Q. *Chem. Mater.* **2007**, *19*, 2372.
(15) Rhee, C. H.; Kim, H. K.; Chang, H.; Lee, J. S. *Chem. Mater.* **2005**, *17*, 1691.
(16) Truffier-Bountry, D.; De Geyer, A.; Guetaz, L.; Diat, O.; Gebel, G. *Macromolecules* **2007**, *40*, 8259.
(17) Chen, W.-F.; Kuo, P.-L. *Macromolecules* **2007**, *40*, 1987.
(18) Jiang, S. P.; Liu, Z.; Tian, Z. Q. *Adv. Mater.* **2006**, *18*, 1068.
(19) Deng, W. Q.; Molinero, V.; Goddard, W. A., III *J. Am. Chem. Soc.* **2004**, *126*, 15644.
(20) Landi, B. J.; Raffaelle, R. P.; Heben, M. J.; Alleman, J. L.; VanDerveer, W.; Gennett, T. *Nano Lett.* **2002**, *2*, 1329.
(21) Wang, J.; Musameh, M.; Lin, Y. *J. Am. Chem. Soc.* **2003**, *125*, 2408.
(22) Olek, M.; Kempa, K.; Jurga, S.; Giersig, M. *Langmuir* **2005**, *21*, 3146.
(23) Liu, J.; Rinzler, A. G.; Dai, H.; Hafner, J. H.; Bradley, R. K.; Boul, P. J.; Lu, A.; Iverson, T.; Shelimov, K.; Huffman, C. B.; Rodriguez-Macias, F.; Shon, Y.-S.; Lee, T. R.; Colbert, D. T.; Smalley, R. E. *Science* **1998**, *280*, 1253.

Experimental Section

Materials. The multiwalled CNTs used in this work were purchased from Desunnano Co. Ltd., Taiwan (purity >95%, length 1−2 μm, diameter 10−20 nm). Poly(oxyalkylene)diamine (JEFFAMINE XTJ-511) was supplied from Huntsman Corp. (3-Glycidoxypropyl)trimethoxysilane (GPTMS) was purchased from Dow Corning Corp. TEOS was from Fluka Corp. Hydrochloric acid (37%) was from Riedel-de Haën. Ethanol and 2-propanol (IPA) were bought from Mallinckrodt. A 20% Nafion DE-2020 dispersion was supplied from DuPont Fluoroproducts. Other chemicals including nitric acid (HNO_3; 69.5 wt %), thionyl chloride ($SOCl_2$), sodium chloride (NaCl), methanol (CH_3OH), and sulfuric acid (H_2SO_4) were obtained from Aldrich. All aqueous solutions were prepared using deionized water purified through a Milli-Q system.

Preparation of CNT-EO. The synthesis of poly(oxyalkylene)-diamine-functionalized carbon nanotubes (CNT-EO) is shown in Scheme 1. The pristine carbon nanotubes were pretreated with HNO_3 at 80 °C for 6 h. After being cooled to room temperature, the reaction mixture was washed with deionized water until a pH of 7 was obtained, subsequent to which the product was dried under vacuum at 60 °C for 24 h, to give carboxyl-functionalized CNTs (CNT-COOH). The prepared CNT-COOH was refluxed with excess neat thionyl chloride at 65 °C for 24 h. The residual $SOCl_2$ was removed by distillation, giving acyl chloride-functionalized CNTs. The acyl chloride-functionalized CNTs were immediately reacted with excess poly(oxyalkylene)diamines (POAs, XTJ-511) at 120 °C for 48 h. The unreacted POA was removed by washing with ethanol and deionized water until the filtrate became clear, yielding CNT-EO.

Preparation of CNT-EO/Nafion and Polysiloxane-Modified CNT/Nafion Membranes. CNT-EO was dispersed in IPA with the aid of ultrasonic agitation for 1 h. Subsequently, different amounts of 20 wt % Nafion DE-2020 dispersion (CNT-EO content (α) = [CNT-EO]/([CNT-EO] + [Nafion solid]); α = 5%, 10%, 15%, and 20% for membranes A, B, C, and D, respectively) were dropped slowly and the resulting solution mixed well. A homogeneous black dispersion was then formed. The solution was then poured onto an aluminum plate followed by slow removal of the solvent at 30 °C for 12 h and drying at 80 °C for 3 h.

Two kinds of polysiloxane-modified samples (membranes C-G and C-GT) were prepared according to the following procedure. CNT-EO was dispersed in IPA with the aid of ultrasonic agitation for 1 h. GPTMS was added to the CNT-EO dispersion with a molar ratio of amine:GPTMS = 1:2 and the resulting mixture stirred at 80 °C for 1.5 h. Nafion DE-2020 dispersion was then dropped slowly and the resulting solution mixed well to form a polysiloxane-modified CNT/Nafion composite (membrane C-G, α = 15%). TEOS was also used to reinforce the silica network. After GPTMS was reacted with CNT-EO, TEOS was then added and the solution hydrolyzed under acidic conditions (amine:GPTMS:TEOS = 1:2:2). The sol−gel process was carried out at room temperature for 1 h. The hydrolyzed solution was then mixed with Nafion DE-2020. These solutions were poured onto an aluminum plate followed by slow removal of the solvent at room temperature for 12 h and curing at 80 °C for 3 h, 100 °C for 2 h, and 120 °C for 1 h.

Characterizations. X-ray photoelectron spectroscopy (XPS) measurements were carried out with a VG Scientific ESCALAB 210 electron spectrometer using Mg Kα radiation under a vacuum of 2×10^{-8} Pa. Narrow-scan photoelectron spectra were recorded for the C 1s, O 1s, N 1s, and Si 2p regions. To compensate for charging effects, binding energies were corrected for covalent C 1s at 284.6 eV after curve fitting.

The morphologies and tube size distributions of the modified CNTs were characterized by transmission electron microscopy

Scheme 1. Illustration of the Synthetic Process Comprising the POA Grafting of CNTs, Covalent Reaction of GPTMS, and Sol−Gel Process of TEOS To Form Polysiloxane-Functionalized CNTs

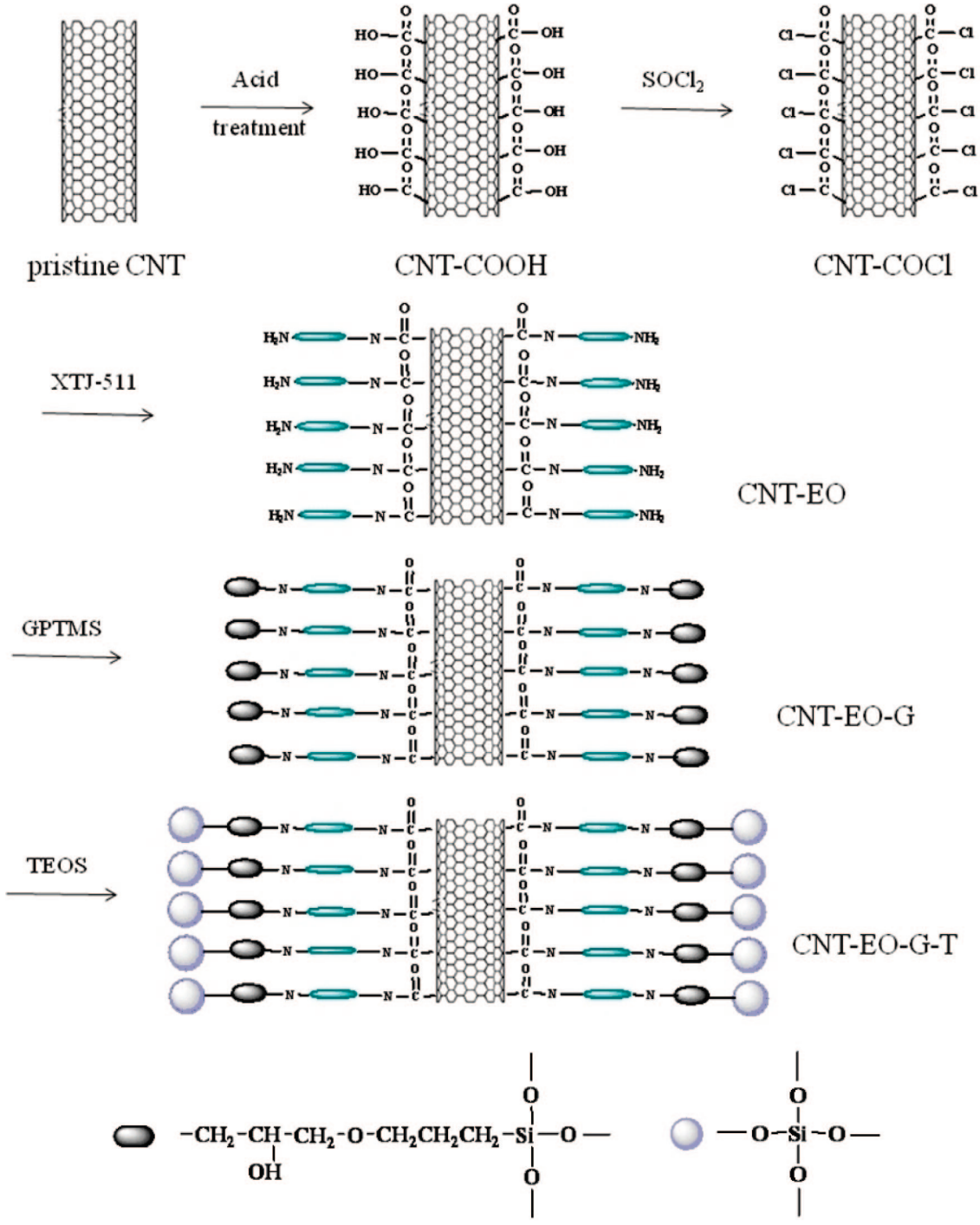

(TEM) using a JEOL JEM-1200CX-II microscope operating at 120 kV. Hitachi S4200 field emission scanning electron microscopy (SEM) was used to observe the cross-section morphology of CNT-EO/Nafion membranes with different CNT-EO contents.

FTIR measurements were recorded on a Nicolet 550 system equipped with an attenuated total reflectance (ATR) accessory for the polymer membranes in the range of 4000−600 cm^{-1}. Each sample was vacuum-dried at 80 °C for 24 h to remove the absorbed water in the sample.

Thermogravimetric analysis (TGA) was performed using a thermogravimetric analyzer (Perkin-Elmer TGA 7) over a temperature range of 50−900 °C at a heating rate of 20 °C/min under a nitrogen atmosphere.

The ion-exchange capacity (IEC) was measured by classical titration. The membranes were soaked in a saturated NaCl solution. Released protons were titrated using 0.05 N NaOH aqueous solution.

Two types of water, freezing and nonfreezing water (bound water), in the membranes were detected by melting transitions in differential scanning calorimetry (DSC) measurements using a DuPont TA2010 differential scanning calorimeter with a low-temperature measuring head and a liquid nitrogen-cooled heating element.[24,25] The samples were first cooled from +25 to −50 °C and then heated at a rate of 5 °C min^{-1} to +40 °C. Calculation of the amount of bulk water in the samples was done by integrating the peak area of the melt endotherm. The degree of crystallinity of

Scheme 2. Proton Conduction in CNT-EO/Nafion and CNT-EO-GT/Nafion Composites

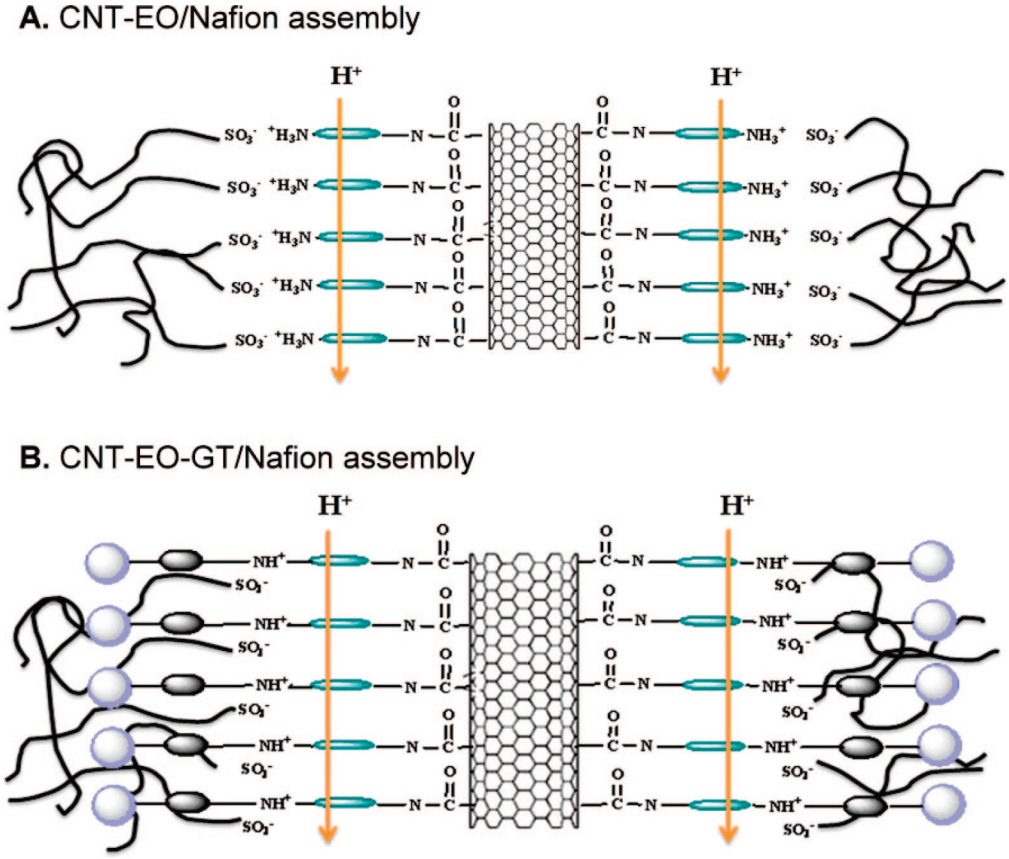

the water, obtained from the heat of fusion of pure ice, 334 J g^{-1}, was used as a standard. An empty aluminum pan was used as a reference.

Proton conductivity of the polymer membranes was measured by an ac impedance technique using an electrochemical impedance analyzer (CH Instrument model 604A), where the ac frequency was scanned from 100 kHz to 10 Hz at a voltage amplitude of 10 mV. Fully hydrated membranes were sandwiched into a Teflon conductivity cell equipped with Au plates. The temperature dependence of proton conductivity was carried out by controlling the temperature from 30 to 95 °C at a relative humidity of 95%. For the measurement at 100−130 °C, the fully moisture-saturated membranes were placed in an oven at 100 °C (no extra gas flow) for at least 3 h. The conductivity was measured every 30 min until it remained at a steady value. Then the conductivities at elevated temperatures (110−130 °C) were measured after the membrane was equilibrated for 1.5 h.

Results and Discussion

Synthesis of Poly(oxyalkylene)diamine-Functionalized Carbon Nanotubes. The incorporation of silica/poly(oxyalkylene) layer-upon-layer structures onto multiwall CNTs involves four main steps based on a "step-by-step graft-to" method as shown in Scheme 1. First, carboxyl-functionalized CNT was prepared by oxidizing CNT (tube diameter ~15 nm) with 60% HNO_3 to produce a significant density of carboxyl groups on the CNT surface,[26] which were then reacted with $SOCl_2$ to produce acyl chloride-functionalized CNT. POA (XTJ-511) was grafted onto the CNT surface by reactions between the acyl chloride residues and the amine groups to form CNT-EO. In this way a black, macroscopically homogeneous dispersion was obtained as CNT-EO in 2-propanol. The materials prepared as dispersions were stable for several days. These grafted amino-terminated chains served in turn as the binding sites for GPTMS. GPTMS can react either with an amine group via oxirane ring cleavage, leading to an organic polymeric network, or with H^+ catalysts via a sol−gel process involving $Si(OR)_3$ groups, leading to the formation of inorganic siloxane chains. This approach has been demonstrated and documented in our recent papers.[27,28] TEOS was also added to construct a robust silica network, which may immobilize the modified CNTs in the Nafion matrix. The so-called "sol−gel" technique is a covalent cross-linking method, which in contrast to the traditional blending method, produces an interconnected porous network in the matrix, thereby preventing the phase separation of silica and the matrix material.

After grafting of POA onto CNT, the total amount of amine groups on the CNT sidewall was determined by a back-titration method to be 1.48 mmol/g of CNT-EO. XPS was employed to elucidate the surface states of these CNTs

(24) Karlsson, L. E.; Wesslén, B.; Jannasch, P. *Electrochim. Acta* **2002**, *47*, 3269.
(25) Nakamura, K.; Hatakeyama, T.; Hatakeyama, H. *Polymer* **1983**, *24*, 871.
(26) Hull, R. V.; Li, L.; Xing, Y.; Chusuei, C. C. *Chem. Mater.* **2006**, *18*, 1780–1788.
(27) Liang, W.-J.; Chen, Y.-P.; Wu, C.-P.; Kuo, P.-L. *J. Phys. Chem. B* **2005**, *109*, 24311.
(28) Kuo, P.-L.; Chen, W.-F.; Liang, W.-J. *J. Polym. Sci., Part A: Polym. Chem.* **2005**, *43*, 3359.

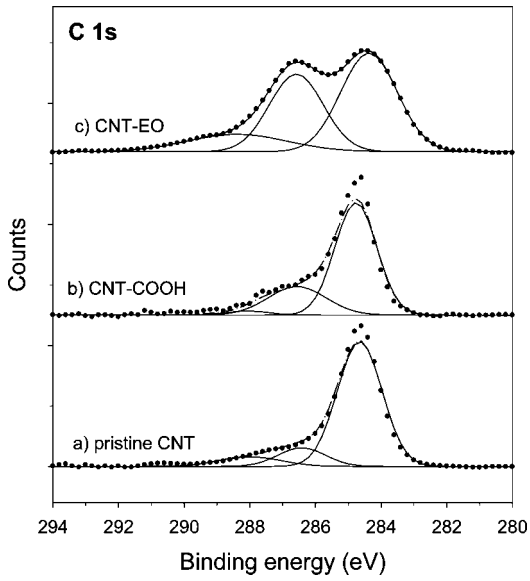

Figure 1. XPS spectra in the C 1s region of: (a) pristine CNT, (b) CNT-COOH, and (c) CNT-EO.

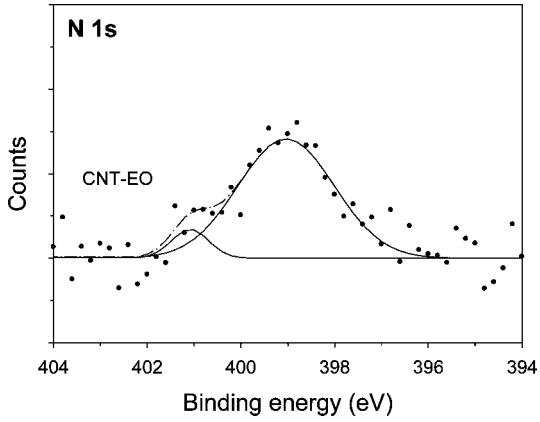

Figure 2. N 1s XPS spectra of the CNT-EO powder.

after modification. Our experimental results confirm the existence of the surface functional groups on these modified materials. The XPS results clearly demonstrate that the carbon nanotubes treated with HNO_3 give oxidized carbon (Figure 1) compared with the untreated sample. In pristine CNT, graphitic carbon at 284.6 eV is detected, which is ascribed to the combination of the sp^2 C═C, sp^3 C−C, and C 1s peaks. Only a trace of oxidized carbon is detected at 286.4 and 288 eV, which can be considered as an adsorbed oxygen species.[29] For the HNO_3-treated CNTs (spectra b, Figure 1), the 286.4 eV peak increases, indicating that a high density of carboxyl groups is produced on the surface of CNT. It can be seen in Figure 1 (spectra c) that the 286.4 eV peak increases markedly after grafting of POA onto the CNT surface. This increase is attributed to the amide linkage, the peak position of which is coincident with that of the C−O−C bonding of the oxyalkylene chain. Derived from the N 1s line shown in Figure 2 are two peaks which appear at 399 and 401 eV; they respectively indicate the presence of free amine groups[30] and the protonated ammonium ions.[31]

The resulting morphology of CNT-EO was investigated by TEM in terms of the quality of the dispersion and the diameter of the nanotubes. The TEM image of the pristine CNT (Figure 3a) shows that the tube diameter is 18.9 nm and that no extra phase or stain was detected on the sidewall. For CNT-EO, POA-coated tubes are clearly produced (Figure 3b). The polymer shell surrounding an individual nanowire is very uniform. The tube is clearly enwrapped by about 2 nm of polymer chains, although the precise boundary between the tube and the polymer layer is somewhat indistinct. The average tube diameter of CNT-EO was calculated as being 23.6 nm. Accordingly, the grafting of POA on the tube wall is evident for CNT-EO with a shell thickness of about 2.3 nm. It can be seen that the nanotubes tend to self-assemble, forming aggregates by the interactions which occur between the POA chains.

Morphology of Functionalized CNT/Nafion Composite Membranes. We performed SEM on the fracture surfaces of the composite membranes. Six images are shown in Figure 4, which compare the morphologies of the composites loaded with pristine CNTs and membranes A, B, C, D, and C-GT. The fracture surface of the composite membrane loaded with the pristine CNTs (CNT content 15%) shows nonuniform dispersion and the tendency for the nanotubes to entangle as agglomerates (Figure 4f). Most of the pristine CNTs show sliding and "pulling-out" at the surface as shown in the inset of Figure 4f, suggesting a limitation of load transfer. By comparison, the CNT-EO system shows good homogeneity and dispersion on the fracture surface. A number of bundles were found to have broken rather than just having been pulled out of the surface, demonstrating that strong interfacial bonding exists between the Nafion matrix and the functionalized nanotubes. As the loading of the CNT-EO increased, good dispersion was still achieved, and most of the CNT-EO is shown to be embedded and tightly held in the matrix (Figure 4a−d). Only some pulled-out CNTs are observed in the case of membrane D due to its high CNT content of 20%. As for the polysiloxane-modified membrane C-GT (Figure 4e), a better dispersion of CNTs is observed than in membrane C, indicating that the polysiloxane network would help immobilize the functionalized CNTs in the Nafion matrix. In addition, it can be observed that the tube diameter of the pulled-out CNTs changed with the CNT content. The tube diameter of the pristine CNT/Nafion composite is 29 nm, and those of membranes A, B, C, and D are 85, 81, 72, and 55 nm, respectively. When the pristine CNT/Nafion membrane was compared with membrane C, it was found that the tube diameter increased from 29 to 72 nm. This can be related to the interaction between CNT-EO and Nafion, which promotes the incorporation of the Nafion onto the CNT's sidewalls. The tube diameter decreased as the CNT-EO content increased, indicating that less Nafion is attached onto CNT-EO at a higher CNT-EO content. These results

(29) Moulder, J. F.; Stick, W. F.; Sobol, P. E.; Bomben, K. D. *Handbook of X-ray Photoelectron Spectroscopy*; Perkin-Elmer: Eden Prairie, MN, 1992.

(30) Sharma, J.; Mahima, S.; Kakade, A. B.; Pasricha, R.; Mandale, A. B.; Vijayamohanan, K. *J. Phys. Chem. B* **2004**, *108*, 13280–13286.

(31) Haimov, A.; Cohen, H.; Neumann, R. *J. Am. Chem. Soc.* **2004**, *126*, 11762–11763.

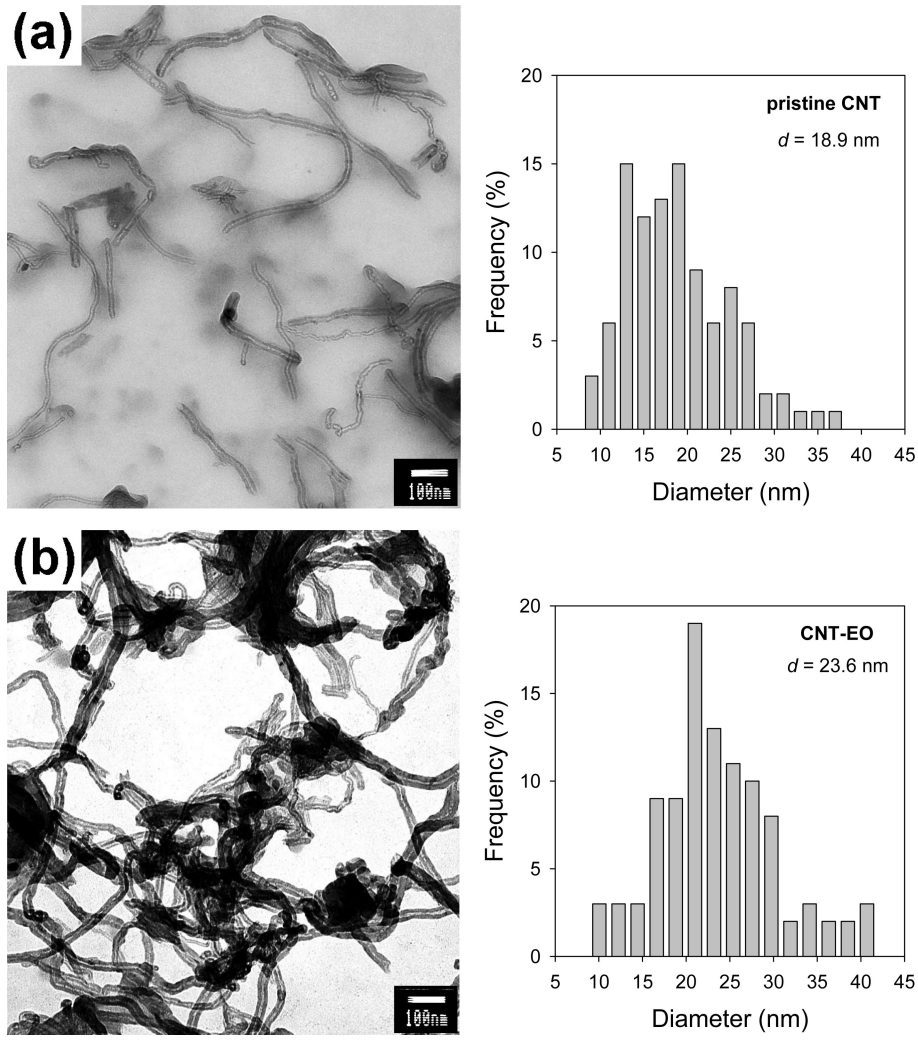

Figure 3. TEM images of (a) pristine CNTs and (b) CNT-EO. The histograms show the particle size distributions.

are related to the interactions between CNT-EO and Nafion, which are examined in the next section by ATR/FTIR and X-ray photospectroscopy.

Interaction between CNT-EO and Nafion. To elucidate the nature of the physical binding of the functionalized CNTs to Nafion, the membranes were probed with ATR/FTIR, XPS, and TGA. ATR/FTIR spectra in the 900−1400 cm^{-1} region are shown in Figure 5. The characteristic absorption bands at 968 and 980 cm^{-1} are ascribed to the symmetric stretching of the −COC− groups, while those at 1057 and 1151 cm^{-1} are assigned to $-SO_3^-$ and $-CF_2-$ symmetric stretching vibrations.[32] The peak at 1215 cm^{-1} consists of two, almost superimposed, bands at 1207 cm^{-1} for the $-CF_2-$ asymmetric stretching vibrations and at 1220 cm^{-1} for the $-SO_3^-$ asymmetric stretching vibrations. The spectra displayed in the inset of Figure 5 show the $-SO_3^-$ symmetric stretching bands. A progression in the maximum of the symmetric stretching bands toward a lower wavenumber is observed as the CNT-EO concentration increases from 1057.2 cm^{-1} of the recast Nafion DE-2020 to 1053.6 cm^{-1} of membrane D. It is known that the shift in the $-SO_3^-$ symmetric stretching peak occurs with a change in the environment around the sulfonic acid groups. For example, the $-SO_3^-$ symmetric stretching peak shifts with a change in the radius of the cation[33,34] or with ionic interactions between the $-SO_3^-$ groups and positively charged functionalities.[35,36] In the present system, the amine groups on CNT-EO interact with the sulfonic acid groups, which in turn decreases the frequency of the $-SO_3^-$ stretching peak. This suggests a weaker polarization of the S−O bond.

The XPS spectra of membranes A and C in the C 1s, O 1s, and N 1s regions and the Si 2s line for membranes C-G and C-GT are shown in Figure 6. When we examine the hybrid process of incorporating CNT-EO into Nafion, the presence of CNT-EO is confirmed by the appearance of the C 1s and O 1s lines in the XPS spectra. In the case of membrane A, the presence of the carbon line at 284.6 eV (Figure 6a), which is attributed to the C−H groups, indicates that CNT-EO has been successfully blended with Nafion. Another component of the carbon line, at 291.5 eV, is

(32) Iwamoto, R.; Oguro, K.; Sato, M.; Iseki, Y. *J. Phys. Chem. B* **2002**, *106*, 6973.
(33) Lowry, S. R.; Mauritz, K. A. *J. Am. Chem. Soc.* **1980**, *102*, 4665.
(34) Lage, L. G.; Delgado, P. G.; Kawano, Y. *Eur. Polym. J.* **2004**, *40*, 1309.
(35) Park, H. S.; Kim, Y. J.; Hong, W. H.; Choi, Y. S.; Lee, H. K. *Macromolecules* **2005**, *38*, 2289.
(36) Tannenbaum, R.; Rajagopalan, M.; Eisenberg, A. *J. Polym. Sci., Part B: Polym. Phys.* **2003**, *41*, 1814.

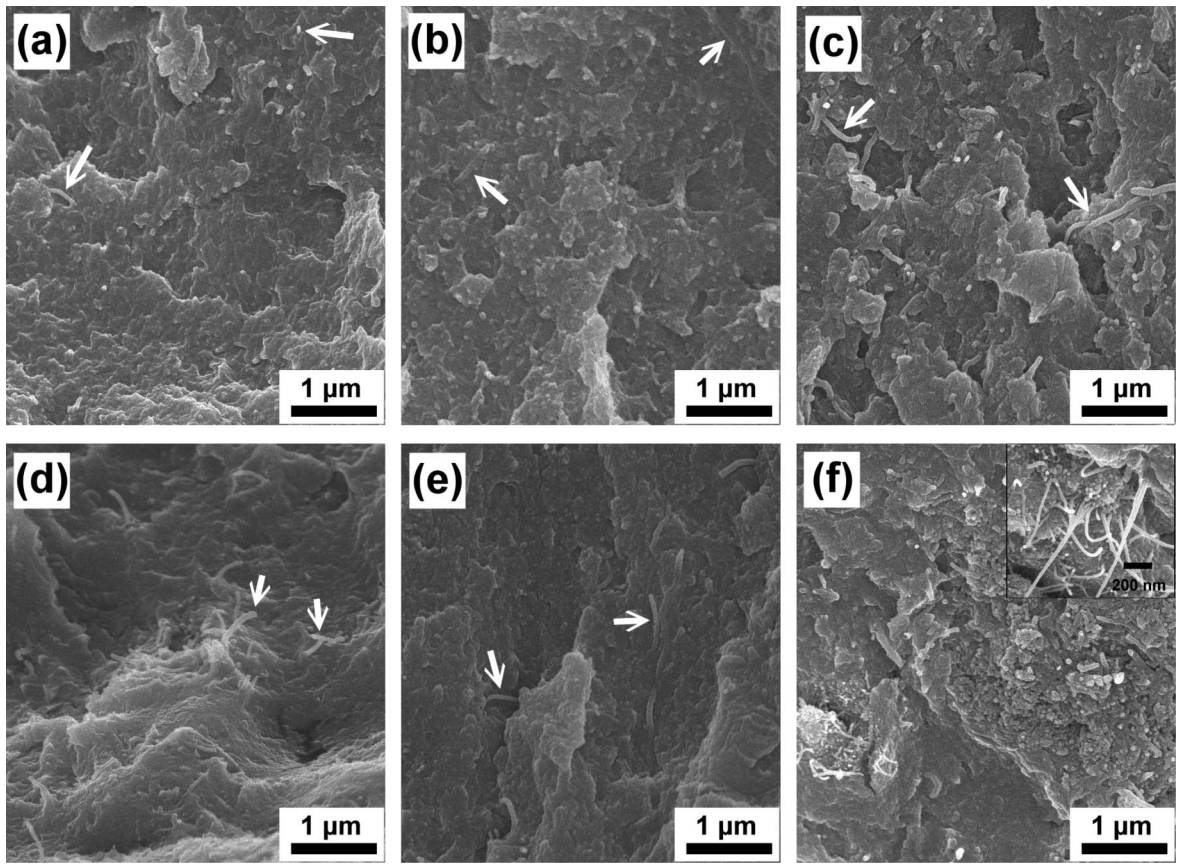

Figure 4. Cross-section images of scanning electron micrographs of (a) membrane A, (b) membrane B, (c) membrane C, (d) membrane D, (e) membrane C-GT, and (f) the pristine CNT-doped membrane.

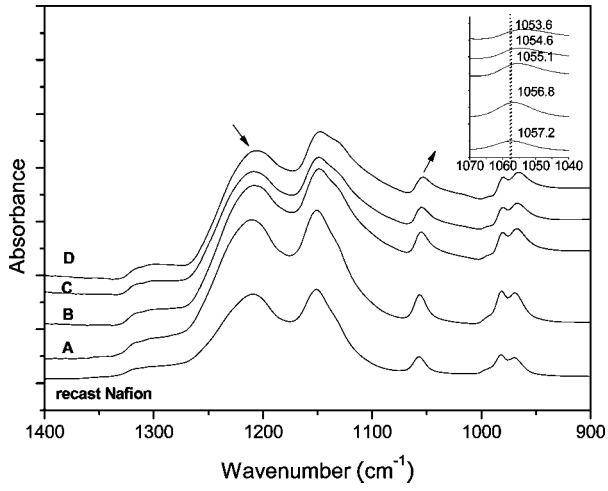

Figure 5. ATR/FTIR spectra of the recast Nafion membrane and the composite membranes: membranes A, B, C, and D. The inset shows the shift of the $-SO_3^-$ symmetric stretching vibrations.

attributed to the fluorinated carbon of Nafion.[37] As the CNT-EO concentration increases, the intensity of the C−H peak increases in comparison with that of the C−F peak. The O 1s line in Figure 6b is found to consist of three signals. The first peak at 535 eV indicates the existence of the $-CF_2SO_3^-$ species. The other two peaks are assigned to carbonaceous species; they include the fluoroether species ($-CF_2-O-$) at about 534 eV and also the ether oxygen species ($-CH_2-O-$) at 531.8 eV. When α increases to 15%, the intensity of the $-CF_2SO_3^-$ peak at 536.8 eV becomes weaker compared with that of the carbonaceous oxygen. The presence of polysiloxane in the membrane is confirmed by the Si 2s lines in the XPS spectra. Figure 6c shows the Si 2s spectra for membranes C-G and C-GT. The peak at 102.4 eV is attributed to Si−O−Si and Si−OH bonding,[38] indicating that polysiloxane has been successfully blended with Nafion.

The ionic interactions between the amine groups on CNT-EO and the sulfonic acid groups on Nafion were detected by the N 1s lines. For membrane C (Figure 6d), the N 1s peak has at least two components found at 400 and 401 eV. These two peaks are both attributed to positively charged nitrogen corresponding to the above ATR/FTIR results. Hence, it is reasonable to explain that the presence of interactions between the $-SO_3^-$ and $-NR_3^+$ functional groups weakens the polarization of the S−O bonds.

TGA was also used to characterize the incorporation of Nafion onto CNT-EO. Figure 7 shows the first derivative of the TG traces of membrane C as well as the recast Nafion fired in N_2. The TG curve of membrane C (see the Supporting Information) shows two apparent decreases in the sample's weight over the temperature ranges 300−380 and 400−550 °C, which is similar to the curve of recast Nafion. As shown

(37) Bae, B.; Kim, D.; Kim, H.-J.; Lim, T.-H.; Oh, I.-H.; Ha, H. Y. *J. Phys. Chem. B* **2006**, *110*, 4240.

(38) Wróbel, A. M.; Walkiewicz-Pietrzykowska, A.; Klemberg-Sapieha, J. E.; Nakanishi, Y.; Aoki, T.; Hatanaka, Y. *Chem. Mater.* **2003**, *15*, 1749.

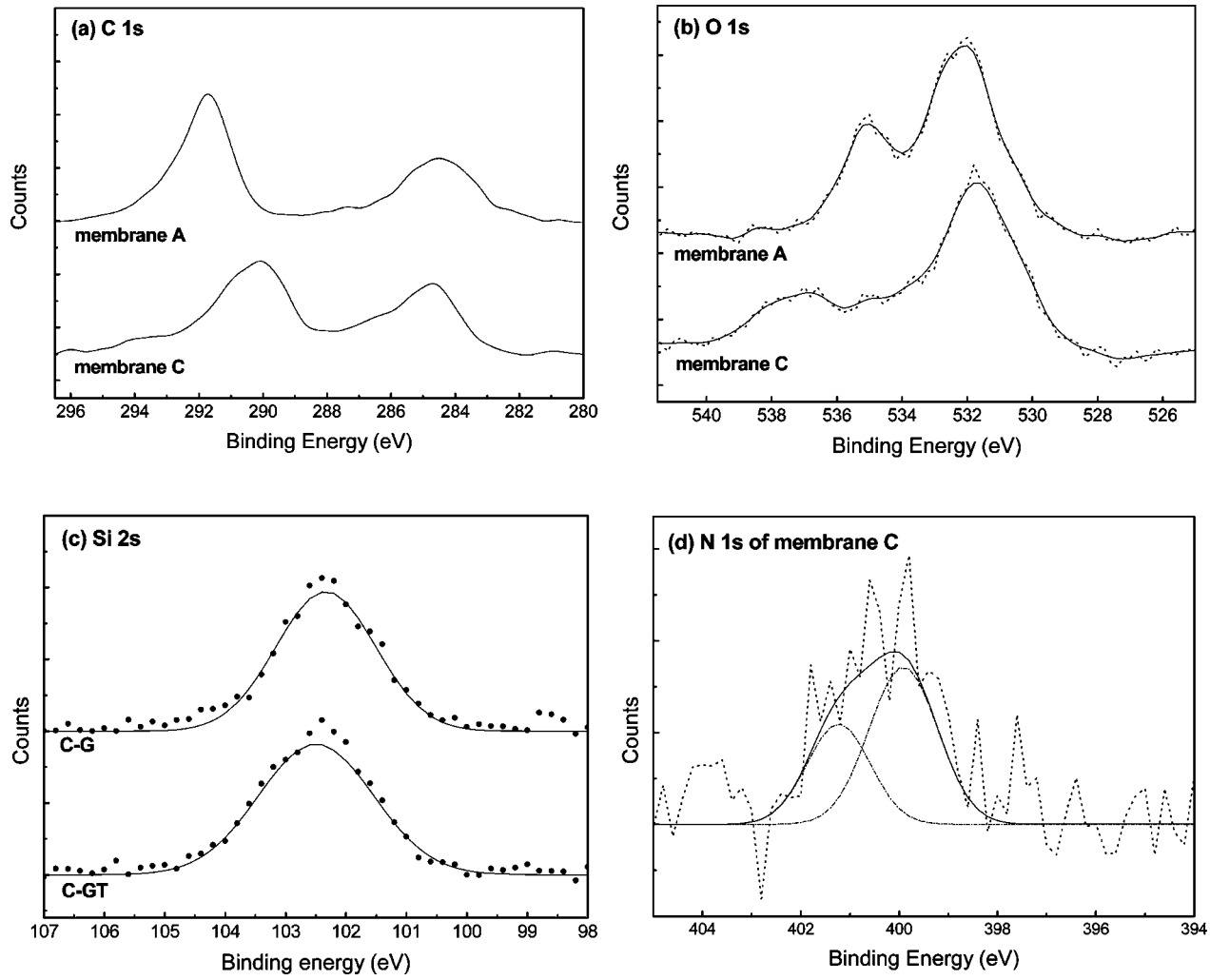

Figure 6. Comparison of the XPS spectra in the (a) C 1s region, (b) O 1s region between membrane A and membrane C, (c) Si 2s region of membranes C-G and C-GT, and (d) N 1s region of membrane C.

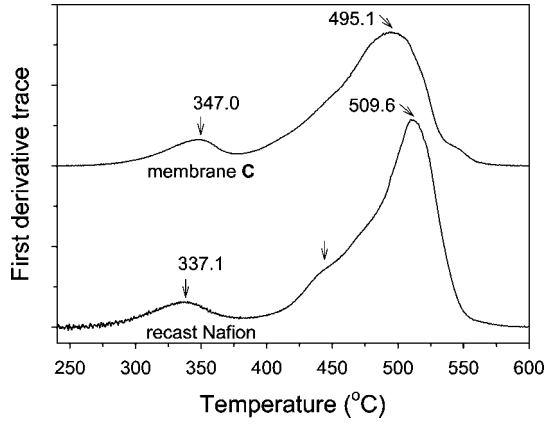

Figure 7. First derivative of TG traces of the recast Nafion and membrane C.

in Figure 7, the decrease in sample weight of recast Nafion produced two main peaks in the first-derivative plot. During the first step, a broad peak centered at 337.1 °C was produced. This weight loss is assigned to a desulfonation process.[39] The second apparent peak was produced between 400 and 550 °C. This stage can be divided into two regions. The shoulder in Figure 7 ranges from 400 to 470 °C and is related to a side-chain decomposition, while the intense peak ranging from 470 to 550 °C corresponds to the decomposition of the Nafion backbone.[40] In the case of membrane C, the peak maximum in the first stage shifted to a higher temperature (347.0 °C) with respect to that found with recast Nafion. This higher temperature discloses a more thermostable sulfonate group in membrane C. We attributed this shift to the intermolecular interaction between $-SO_3^-$ and $-NH_3^+$ that potentially retards the degradation of sulfonate groups. We postulated that it is possible that the ionic interactions between the amine groups of CNT-EO and the sulfonate groups of Nafion disrupted the desulfonation process and side-chain decomposition.[41] In the second stage, the decomposition of the polymer's backbone is strongly related to the degree of crystallinity of the Nafion matrix. The decomposition temperature of this peak for membrane C (495.1 °C) is lower than that of the recast Nafion (509.6 °C), indicating that the crystallinity of C is lowered following the addition of CNT-EO.

(39) Miyatake, K.; Oyaizu, K.; Tsuchida, E.; Hay, A. S. *Macromolecules* **2001**, *34*, 2065.
(40) Almeida, S. H.; Kawano, Y. *J. Therm. Anal. Calorim.* **1999**, *58*, 569.
(41) Park, H. S.; Kim, Y. J.; Hong, W. H.; Lee, H. K. *J. Membr. Sci.* **2006**, *272*, 28.

Table 1. Electron Conductivity of the Pristine, Modified CNT and the Nanocomposite Membranes

sample	electron conductivity (S/cm)
pristine CNT powder	1.45
CNT-EO powder	0.4
CNT-EO-G powder	0.038
CNT-EO-GT powder	0.016
recast Nafion DE-2020 membrane	2.3×10^{-6}
membrane C	1.0×10^{-6}
membrane C-G	1.4×10^{-8}
membrane C-GT	1.0×10^{-9}

As a result, the invasion of CNT-EO into the cluster is able to stabilize the polar phase by means of the interactions between Nafion and CNT-EO and thereby decrease the crystallinity of the backbone indirectly due to the disruptive effect of swollen clusters on the lamellar ordering of the nonpolar backbone.[42]

Water Uptake. The water uptake in a proton-conducting membrane is an important factor that directly affects proton transportation in proton-conducting membranes. Generally, it is believed that protons can be transported along with cationic mixtures such as H_3O^+ and $H_5O_2^+$ in the aqueous medium. In a fully hydrated state, sulfonated polymers may dissociate immobile sulfonic acid groups and mobile protons in aqueous solution. Then the free protons move through a localized ionic network within fully water-swollen sulfonated polymer membranes. Accordingly, an appropriate water content level should be maintained in sulfonated polymer membranes to guarantee high proton conductivity.

The measured water uptakes of the functionalized CNT/Nafion composite membranes (at 30 °C), either with various CNT-EO concentrations, or with different functionalizations, after immersion in water, are compared in Table 2. It is worth noting that all the membranes have lower water uptakes than Nafion-117. One might ascribe this lower water uptake to the lower IEC value of the CNT-EO/Nafion membrane. Membranes A and B have IEC values of 0.96 and 0.89 mequiv/g, respectively, which are higher than, or close to, that of Nafion-117. Therefore, the much lower water uptake can be ascribed to the fact that ionic interaction between CNT-EO and Nafion markedly reduces the swelling and/or that the CNTs occupy the volume available for water absorption.

Comparing membrane C-G with membrane C (ω_t = 13.2%), membrane C-G had a higher water uptake of 16.6%. The larger sorption of water may be caused by the higher concentration of hydrophilic components in the matrix; i.e., the epoxide chains and siloxane networks may provide a more hydrophilic domain and facilitate greater interaction, resulting in the adsorption of more water. For the silica-reinforced C-GT membrane, the observed water uptake was lower than that of membranes C and C-G. We attribute this low water uptake to the robust scaffold that was produced by the incorporated silica framework, which reduced the vacant space available for accommodating water in the membrane.

State of Water. Water sorption characteristics are of great importance for proton-conducting polymer membranes. The states of water such as free water and bound water in sulfonated polymers directly affect the transportation of protons across the membranes. The DSC thermograms of the fully hydrated membranes (Figure S2, Supporting Information) show that all the samples had a broad endothermic peak which consisted of two major melting peaks. The peaks corresponded to freezable water including free water at approximately −2 °C and loosely bound water at approximately −5 to −30 °C. The membranes with higher CNT-EO concentrations clearly showed a lower melting point. The association of water molecules with other species such as ionic and polar groups or its confinement in nanosized domains dominated the thermal transitions of water molecules. The melting point (T_m) of water for all the composite membranes as well as Nafion-117 is displayed in Table 3. For perfluorinated polymers, the increasing interaction between the membranes and the adsorbed water is responsible for the left shift of the melting peak. In the case of the CNT-EO/Nafion membranes, those that have a higher CNT-EO concentration also possess a lower T_m. Since there are two kinds of water in membranes corresponding to free water around −2 °C and loosely bound water around −5 to −30 °C, the decreasing T_m with increasing CNT-EO concentration can be attributed to the increasing percentage of bound water.

The weight fraction of free water (ω_f) in the fully hydrated membranes can be estimated from the total melting enthalpy (ΔH_m) that is obtained by integration of the transition heat capacity (ΔC_P) over the broad melting temperature interval in

$$\omega_f = \frac{\Delta H_m}{Q_{melting}} = \frac{\int \Delta C_P \, dT}{Q_{melting}}$$

where $Q_{melting}$ is the heat of fusion of bulk ice (334 J/g). The weight fraction of bound water (ω_b) is calculated by subtracting the amount of freezing water (ω_f) from the total water uptake (ω_t). Then the bound water degree ($\chi = \omega_b/\omega_t$) is calculated from the ratio of the amount of bound water to the total water uptake. Table 3 also summarizes the amount of freezing water and bound water and the corresponding bound water degree. For CNT-EO/Nafion composite membranes, an increase in CNT-EO concentration results in a decrease in ω_f. As described previously in the FTIR and XPS experiment, the CNT-EO/Nafion matrixes contain other polar functional groups such as the $-SO_3^-NH_3^+-$ and $-COC-$ groups from the modified CNT surface. In addition to the strong interaction between the water and the sulfonic acid groups, there are enough binding sites in the membranes to constrain water on the CNT sidewalls and thus bring about a high ω_b. An increase in the α value also induced an increase in the bound water degree (χ) from 64.7% to 92.0%. For the polysiloxane-functionalized membranes, membranes C-G and C-GT, there exists a high bound water degree (~95%). Compared with sample C, membrane C-G has the same T_m value with a higher water uptake, while membrane C-GT has a higher T_m with a water uptake close to that of sample C. This result indicates that the incorporation of a silica matrix in the silica-reinforced membrane C-GT changed the environment of adsorbed water and decreased the intensity of water binding. The high bound water degree (94.6%) of

(42) Moore El, B. R.; Martin, C. R. *Macromolecules* **1989**, *22*, 3549.

Table 2. Water Uptake and Proton Conductivity at Different Temperatures of the Functionalized CNT/Nafion Composite Membranes

sample	CNT-EO content, α (wt %)	IEC (mequiv/g)	water uptake, ω_t[a] (wt %)	proton conductivity, σ (10^{-2} S/cm) 30 °C[b]	95 °C[b]	130 °C[c]
Nafion-117		0.91	24.3	3.3	4.1	0.0016
A	5	0.96	19.0	3.5	5.3	0.069
B	10	0.89	17.8	2.8	6.5	0.14
C	15	0.85	13.2	2.2	8.6	0.9
D	20	0.79	15.0	2.8	9.3	6.3
C-G	15	0.74	16.6	1.4	7.8	0.23
C-GT	15	0.65	12.9	0.93	2.4	0.11

[a] Measured after immersion in water. [b] At 95% RH. [c] At dry conditions.

Table 3. State of Water in CNT-EO/Nafion Ionomers

sample	T_m[a] (°C)	water uptake, ω_t (wt %)	freezing water weight fraction, ω_f (wt %)	bound water weight fraction, ω_b (wt %)	bound water degree, χ[b] (%)
Nafion-117	−2.8	24.3	9.8	14.5	59.7
A	−3.4	19.0	6.7	12.3	64.7
B	−10.8	17.8	4.2	13.6	76.4
C	−17.2	13.2	0.4	12.8	97.0
D	−20.8	15.0	1.2	13.8	92.0
C-G	−17.2	16.6	0.7	15.9	95.9
C-GT	−10.0	12.9	0.7	12.2	94.6

[a] Melting temperature of free and loosely bound water. [b] $\chi = \omega_b/\omega_t$.

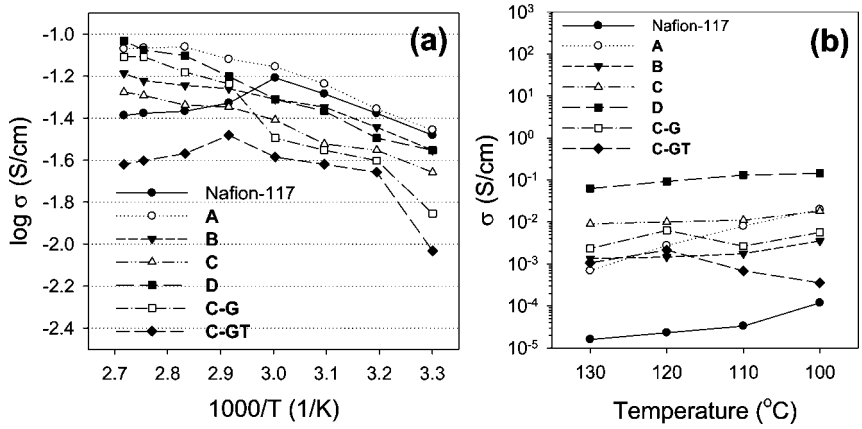

Figure 8. Temperature dependence of proton conductivity for CNT-EO membranes: (a) from 30 to ~95 °C and (b) from 100 to ~130 °C.

membrane C-GT revealed that water was confined within the silica matrixes, which can aid in the conduction of proton at high temperatures.

Electron and Proton Conductivity Measurements. It is known that the electron conductivity of a CNT/polymer composite is significantly raised as the CNT content increases. In the present system, however, the electron conduction is supposed to be hampered. This organic−inorganic layered structure may form a resistance, which effectively inhibits electron conduction between the nanotubes. Table 1 shows the electron conductivity of the functionalized CNTs and the composite membranes. The functionalization of CNTs with POA decreases the electron conductivity from 1.45 S/cm (pristine CNTs) to 0.4 S/cm (CNT-EO powder). After the attachment of a polysiloxane layer and silica shell, the electron conductivity decreased to 0.038 and 0.016 S/cm for CNT-EO-G powder and CNT-EO-GT powder, respectively. This reveals that the layer-upon-layer organic−inorganic shells block the conduction of electrons effectively. For membrane C, the electron conductivity is 10^{-6} S/cm, which is similar to that of the recast Nafion DE-2020 membrane. It was found that the electron conductivity decreased significantly for membranes C-G (1.4×10^{-8} S/cm) and C-GT (1.0×10^{-9} S/cm). Evidently, the coverage of the organic poly(oxyalkyl) chains and the inorganic SiO_2 layers brought about ultralow electron conductivity.

The temperature dependence of proton conductivity (σ) of the CNT-EO/Nafion and polysiloxane-modified CNT/Nafion membranes is shown in Figure 8. Figure 8a shows the conductivity at temperatures ranging from 30 to 95 °C. The change in conductivity with temperature is consistent with the Arrhenius relationship for all the composite membranes. The small slope of the conductivity curve indicates that protons transfer with a low activation energy. We ascribed this low activation energy for proton conduction to the formation of water passage along the CNT-EO sidewall. The surface area of the CNT is 100 m^2/g, so that the surface density is 9.22 units/nm^2. The average distance between the graft chains is 3.7 Å. These closely assembled grafted chains facilitate the binding of water so as to form a continuous water passage and also an $-NH_3^+SO_3^-$ ionic pathway for proton transportation along the carbon tube's wall.

In general, the proton conductivities of the CNT-EO/Nafion membranes decrease with an increasing CNT-EO concentration due to the decrease in ion exchange capacity and the total water uptake. It is obvious that the conductivity above 60 °C of Nafion-117 decreased; however, the conductivity of these composite membranes did not decline, but instead increased, with the exception of membrane C-GT. It is interesting to find that the proton conductivity of membrane D is higher than that of Nafion-117 at 95 °C, while the opposite is true at 30 °C. The lower proton conductivity of membrane D at 30 °C can be ascribed to its lower IEC value compared to that of Nafion-117. It is found that the T_m of water in membrane D (−20.8 °C) is much lower than that in Nafion-117 (−2.8 °C). This indicates that the interaction between water and membrane D is much stronger than that between water and Nafion-117, which is capable of maintaining bound water as the temperature is raised to 95 °C, resulting in the higher proton conductivity over that of Nafion-117.

As for the GPTMS-modified membrane C-G, the conductivity depended significantly on the temperature. As shown in Table 2, its conductivity at 30 °C (0.014 S/cm) is lower than that of Nafion-117 (0.033 S/cm) and that of membrane C (0.022 S/cm), while at 95 °C (0.078 S/cm) it becomes similar to that of membrane C (0.086 S/cm) and much higher than that of Nafion-117 (0.041 S/cm). This indicates that the proton conduction mechanism appears to change as polysiloxane is incorporated. Here protonic transport occurs via a mixture of both Grotthus- and vehicle-type conduction, where polyatomic molecules such as $H_{2n+1}O_n^+$ are the dominant charge carriers and play a role different from that in the Grotthus-type mechanism. In addition, with further combining of a silica framework in the membrane (curve C-GT in Figure 8a), proton conduction was obstructed. Although the proton conductivity at 70−95 °C became much lower than that of Nafion-117, it was still maintained above 10^{-2} S/cm.

Figure 8b shows the proton conductivity at temperatures ranging from 100 to 130 °C in a dry atmosphere. The conductivity of Nafion-117 decreased markedly to 10^{-5} S/cm, due to a serious loss of water. All the CNT-EO/Nafion membranes have higher proton conductivities than Nafion-117. It is interesting to find that the conductivities of membranes C and D are close to or higher than 10^{-2} S/cm at the relatively high temperature of 130 °C (Table 2). At temperatures higher than 100 °C, mainly the binding strength of water and the sites of the water to be bound are affecting the proton conduction. The IEC value becomes a minor factor. In CNT-EO/Nafion membranes, there are three kinds of binding sites for water, including $-SO_3H$, $-CH_2CH_2O-$, and $-SO_3^-NH_3^+-$ linkages. Membrane A showed a higher proton conductivity at 100 °C than the other membranes and a decreasing conductivity from 100 to 130 °C. It is found that the T_m of water in membrane A (−3.4 °C) is similar to that in Nafion-117 (−2.8 °C). This indicates that the interaction between water and membrane A is not strong enough to maintain the bound water as the temperature is raised. The decreasing curve of conductivity for membrane A can be attributed to the decreasing bound water (mostly bound with -SO_3H) at increasing temperature. Comparatively, membranes B, C, and D showed steady conductivity. We have shown that the binding of water on $-CH_2CH_2O-$ and $-SO_3^-NH_3^+-$ linkages was much stronger than on the $-SO_3H$ group, demonstrated by the T_m in the DSC experiments. Thus, the steady conductivity of membranes B, C, and D can be ascribed to the stronger binding of water inside the membranes. It is also found that the conductivity increased from membrane B to membrane D. The reason for this trend is that the membrane with a higher CNT-EO concentration provides more pathways for proton conduction, possesses higher bound water content, and has a stronger binding strength for water to keep bound water from evaporation.

Table 4. Oxidative Stability of the Functionalized CNT/Nafion Composite Membranes and Nafion-117

ionomer	loss, *l* (wt %)	residue content after testing (wt %)
Nafion-117	1.1	98.9
A	0.4	99.6
B	1.1	98.9
C	1.7	98.3
D	2.6	97.4
C-G	3.7	96.3
C-GT	3.2	96.8

When compared with membrane C (9.0×10^{-3} S/cm), the polysiloxane-functionalized membranes C-G and C-GT were shown to possess a lower conductivity (2.3×10^{-3} and 1.1×10^{-3} S/cm, respectively) at 130 °C. This result can also be ascribed to the existence of the silica framework, which slightly interrupts proton transportation though the bound-water layer. It is well-known that, when the temperature is raised, molecular diffusion results in fast proton conduction. As for membrane C, the binding between $-SO_3^-$ and $-NH_3^+$ along the carbon nanotube is thought to establish an interconnected hydrophilic channel (as shown in Scheme 2), which may provide a more continuous pathway for rapid proton transfer kinetics and for water to diffuse more easily through the water channel at higher temperatures.

Oxidation Stability. The oxidative stability of the hybrid membranes was evaluated in Fenton's reagent at 80 °C for 1 h as an accelerated test. Losses of weight for all membranes after the testing are shown in Table 4. Nafion-117 showed a good resistance against oxidation. The residue percentage of the hybrid membranes decreased as the CNT-EO content increased. The oxidative attack on the membranes by $HO^\bullet$ and $HOO^\bullet$ radical species should mainly occur in the proximity of water-containing hydrophilic domains and on the electron-donating functional groups such as ether and amide groups. All of the hybrid membranes retained more than 96% of their original weight after testing to be acceptable for application.

Conclusions

The aim of the present work was to study the modification of carbon nanotubes by a step-by-step graft-to method for preparing a new type of organic−inorganic hybrid polymer nanocomposite comprising Nafion as a proton donor. Hydrophilic poly(oxyalkylene) was successfully grafted onto the CNTs via a covalent amide linkage, forming amine-functionalized tube walls via a sol−gel process, generating

a polysiloxane framework. The functionalized CNTs can be incorporated into Nafion composites through the ionic interactions between the amino moieties of the CNTs and the $-SO_3H$ groups of Nafion. Furthermore, the functionalized CNT/Nafion nanocomposites possess a superior proton-conducting ability, which suggests they have potential as electrochemical electrolyte membrane materials, or they may serve as functional sensor materials, especially in applications at higher temperatures.

Acknowledgment. We gratefully acknowledge the National Science Council, Taipei, Taiwan, for their generous financial support of this research.

Supporting Information Available: Figures showing the TGA thermogram (Figure S1) and DSC spectra (Figure S2). This material is available free of charge via the Internet at http://pubs.acs.org.

CM8001354